PHYSICAL REVIEW E **74**, 041407 (2006)

Dynamic structure and cluster formation in confined nanofluids under the action of an external force field

Philippe Ben-Abdallah[*]
Laboratoire de Thermocinétique, CNRS UMR 6607, Ecole Polytechnique de l'Université de Nantes, 44 306 Nantes cedex 03, France

(Received 28 June 2006; revised manuscript received 16 August 2006; published 30 October 2006)

The dynamic structure and the formation of clusters in nanoparticle colloidal solutions (nanofluids) confined between two parallel walls and submitted to the action of an external force field is studied by extensive Brownian-dynamics simulations. The self-correlation of individual particles and the time correlation between distinct particles are analyzed by calculating the density-density time correlation (van Hove) function. It is shown that the self-diffusion is reduced by the external force field while the lifetime of collective modes of nanoparticles (i.e., natural phonons) is significantly enhanced by this force. We demonstrate that this result is related to disorder-order transitions in the nanoparticle spatial distribution under perturbation. Interestingly, we highlight that the interaction forces mediated by the walls act like repulsive interparticle forces. They tend to increase the structural disorder and to lower the lifetime of collective modes. Our results suggest that the heat transport properties of nanofluids could be actively controlled in nanometer-size systems.

DOI: 10.1103/PhysRevE.74.041407 PACS number(s): 82.70.−y, 65.20.+w, 65.80.+n, 83.10.Mj

I. INTRODUCTION

Nanofluids [1,2] are liquids containing suspended nanometer-size solid particles. Many of these colloidal suspensions have displayed [1,3,4] in many circumstances an anomalously high thermal conductivity that the classical theory of effective media [5] fails to explain. This unexpected result has caused a strong interest in the scientific community (see Refs. [6,7] for a recent review) because it paves the way to a wide variety of potential applications ranging from transportation and energy production to promising fluidic cooling technologies. Considerable efforts have been, since then, devoted both theoretically and experimentally, in order to understand the origin of this effect. Today, this task remains a challenging problem and only partial conclusions have been reached. Nevertheless, recently a significant conceptual advance has been carried out by Vladkov and Barrat [8]. These authors have demonstrated, using molecular dynamic simulations, that only collective effects to explain the heat transfer enhancement observed in these media.

Among these effects we can identify those related to the self-ordered motions of nanoparticles in the host fluid (i.e., the so-called "natural phonons" which are due to collective motions of particles in the host fluid) and those associated to electrostatic interactions between proximal nanoparticles. Recently, we have shown [9] that the heat exchanges due to near-field interactions between nanoparticles were not able to explain the 10% or larger increases of the thermal conductivity measured [1] in weakly concentrated nanofluids. Therefore, the natural phonons probably must play a major role in the transport of heat through nanofluids. In the present paper we question the possibility of controlling the self- and especially the interparticle correlations of nanoparticles (i.e., the dynamic of individual particles and that of natural phonons) in confined geometries from an external actuation. The ability to individually manipulate nanoparticles in suspension in micro- and nanochannels has been already demonstrated [10,11] in the past. Here, we pursue this work by studying the dynamic structure of colloidal particles under the action of an external force field. For this purpose we calculate the density-density time correlation function of nanoparticles and use its decomposition into a self- and distinct part to study first the self-diffusion and finally the self-ordered motion (natural phonons) of particles in the host fluid.

II. BROWNIAN DYNAMICS MODEL

Let us start by describing the system we consider in this study. It consists of N identical, spherical, Brownian particles of radius R dispersed at positions $(\boldsymbol{r}_1, \boldsymbol{r}_2, \ldots, \boldsymbol{r}_N)$ between two parallel walls in a viscous incompressible solvent made with infinitely smaller molecules (i.e., $r_{fluid} \ll R$). In this system, the short-range repulsive interaction and the van der Waals (vdW) attraction between particles i and j are modeled by a truncated shifted and smoothed Lennard-Jones (TSSLJ) potential

$$u(r_{ij}) = \begin{cases} V_{LJ}(r_{ij}) - V_{LJ}(r_c) - \left(\dfrac{dV_{LJ}}{dr_{ij}}\right)_{r_{ij}=r_c}(r_{ij}-r_c) & r_{ij} \leqslant r_c, \\ 0 & r_{ij} > r_c, \end{cases} \quad (1)$$

where $V_{LJ}(r_{ij}) = 4\varepsilon\left[\left(\frac{\sigma}{r_{ij}}\right)^{12} - \left(\frac{\sigma}{r_{ij}}\right)^{6}\right]$ is a 12-6 LJ potential, $r_{ij} = |\boldsymbol{r}_j - \boldsymbol{r}_i|$ stands for the interparticle distance while r_c, ε, and σ represent the cutoff radius of the TSSLJ potential and the LJ parameters, respectively. All particles also interact with the walls located at $z = \pm h/2$ via the purely repulsive soft potential

---

[*] Electronic address: pba@univ-nantes.fr

1539-3755/2006/74(4)/041407(5)

$$u_{wall}(z) = \begin{cases} \alpha\tilde{\varepsilon}\left[\left(\dfrac{\tilde{\sigma}}{h/2-|z|}\right)^{10} - \left(\dfrac{\tilde{\sigma}}{h/2-|z|}\right)^{4}\right] & |z| \leqslant \gamma, \\ 0 & |z| > \gamma, \end{cases} \tag{2}$$

where $\gamma=\frac{h}{2}-(\frac{5}{2})^{1/6}\tilde{\sigma}$. Here h is the separation distance between the upper and lower surfaces, $\alpha=(\frac{1}{z_{\min}})^{10}-(\frac{1}{z_{\min}})^{4}$ and $z_{\min}=(5/2)^{1/6}\tilde{\sigma}$ are the positions where u_{wall} reaches its minimum value. This choice of potential forbids the sticking of particles on the channel walls. In order to avoid the presence of discontinuity in the force of interaction with the walls and to remove numerical instability in the equation of motion a truncated shifted and smoothed version of u_{wall} has been used in all our simulations.

Also an external force field is applied on the colloidal suspension from the sides of the channel. This force results for instance from an external electromagnetic field induced by a laser irradiation or by a spatial distribution of electrodes. Here we assume this force derivates from the following potential:

$$V_{ext}^{Sym}(z) = \begin{cases} \hat{\varepsilon}\left[\exp\left[\dfrac{2}{h}\left(z-\dfrac{h}{2}\right)\right] + \exp\left[-\dfrac{2}{h}\left(z+\dfrac{h}{2}\right)\right]\right] & |z| \leqslant h/2, \\ 0 & |z| > h/2, \end{cases} \tag{3}$$

which mimic well the Lorentz forcelike potential for a symmetrical electromagnetic irradiation. The translational dynamic of particles in the host fluid is then described by the N-body Langevin equation

$$m\dot{\boldsymbol{v}}_i = -\xi_{ij}\boldsymbol{v}_j + \boldsymbol{F}_i + \underline{\underline{\boldsymbol{\alpha}}}_{ij}\boldsymbol{f}_j, \tag{3'}$$

where $\boldsymbol{v}_i$ is the linear velocity of the particle i, $\bar{\bar{\xi}}$ is the $(3N\times 3N)$ friction tensor, $\boldsymbol{F}_i$ is the sum of interparticle and wall-particle forces acting in the ith particle while $\boldsymbol{f}_j$ represents here a Gaussian field with zero mean and covariance $\langle \boldsymbol{f}_i(t)\boldsymbol{f}_j(t')\rangle = 2\delta_{ij}\delta(t-t')$. According to the fluctuation dissipation theorem [12], the random force $\bar{\bar{\boldsymbol{\alpha}}}_{ij}\boldsymbol{f}_j$ exerted on the particle by the surrounding fluid is related to the friction tensor by the relation $\xi_{ij}=(k_BT)^{-1}\Sigma_l\alpha_{il}\alpha_{jl}$. The system of coupled equations (3) might be solved using the Ermak and McCammon algorithm [13]. This leads to the discrete relation

$$\mathbf{r}_i(t+\delta t) = \mathbf{r}_i(t) + \frac{1}{k_BT}\sum_{j=1}^{N}\mathbf{D}_{ij}(t)\mathbf{F}_j(t) + \delta\hat{\mathbf{r}}_i, \tag{4}$$

where $\delta\hat{\mathbf{r}}_i$ denotes the N-correlated displacement vector and $\bar{\bar{\mathbf{D}}}_{ij}$ is the Kirkwood diffusion tensor which describes the hydrodynamic interactions in the host fluid which is related to the friction tensor by the simple relation $\Sigma_j D_{ij}\xi_{jl}=k_BT\delta_{il}$. In order to satisfy the assumptions of the Ermak and McCammon algorithm, a time step δt is chosen much smaller than the Brownian time (i.e., time necessary for a nanoparticle to move through a distance equivalent to its diameter) and much greater than the momentum relaxation time [i.e., time interval Δt beyond which the velocity $v_i(t+\Delta t)$ of a particle is uncorrelated with the velocity $v_i(t)$]. In our simulations, these conditions are always fulfilled because there are at least two or three orders of magnitude between both characteristic times. The diffusion tensor $\bar{\bar{\mathbf{D}}}_{ij}$ is approximated by the (positive-definite) Rotne-Prager [14] expression

$$\boldsymbol{D}_{ij} = \begin{cases} \dfrac{k_BT}{6\pi\eta R}\bar{\bar{\mathbf{I}}} & (i=j), \\ \dfrac{k_BT}{6\pi\eta r_{ij}}\left[\left(\bar{\bar{\mathbf{I}}} + \dfrac{\boldsymbol{r}_{ij}\otimes\boldsymbol{r}_{ij}}{r_{ij}^2}\right) + \dfrac{2R^2}{r_{ij}^2}\left(\dfrac{1}{3}\bar{\bar{\mathbf{I}}} - \dfrac{\boldsymbol{r}_{ij}\otimes\boldsymbol{r}_{ij}}{r_{ij}^2}\right)\right] & (i\neq j). \end{cases} \tag{5}$$

In this expression η represents the viscosity of host fluid, $\bar{\bar{\mathbf{I}}}$ is the unit dyadic tensor, and $\mathbf{r}_{ij}$ is the vector which relates the center of particle j to the center of particle i. In order for the dynamics to satisfy the fluctuation-dissipation theorem, the stochastic displacement vector in relation (4) must verify the supplementary constraints $\langle\delta\hat{\boldsymbol{r}}_i\rangle=0$ and $\langle\delta\hat{\boldsymbol{r}}_i\delta\hat{\boldsymbol{r}}_j\rangle=2\boldsymbol{D}_{ij}\delta t$.

All our simulations are started with an fcc configuration and the system is equilibrated with at least 30 000 time steps. The duration of this equilibration phase is *a posteriori* checked from the relaxation curve of the cohesion energy (not plotted here). The dynamic properties (van Hove function, viscosity, etc.) are calculated with at least 1000 supplementary time steps. Periodic boundary conditions were applied in the x and y directions parallel to the walls and calculations are carried out with adimensioned variables built from the following references quantities: length $r^*=2R$, temperature $T^*=\varepsilon/k_B$, mass of particles $m^*=m$, dynamic viscosity $\eta^*=(m\varepsilon)^{1/2}/(4R^2)$, time $t^*=2(mR^2)^{1/2}/\varepsilon$, and diffusion $D_{ij}^*=2(\varepsilon.R^2/m)^{1/2}$. The values of the dynamic viscosity, temperature, mass density of particles, and of the volume fraction of nanoparticles used in our simulations are $\eta=159\times10^{-4}$ N.s.m^{-2} (ethylene glycol viscosity), $T=300$ K, $\rho=3970$ kg m^{-3} (aluminum density), and $\phi=1\%$, respectively. The potential parameters used in the present work are $\varepsilon=5k_BT$, $\tilde{\varepsilon}=0.01\varepsilon$, $\sigma=\tilde{\sigma}=d$, and $r_c=1.5\sigma$. The number N of Brownian particles in the simulation boxes is fixed to 108. In confined geometry this number is large

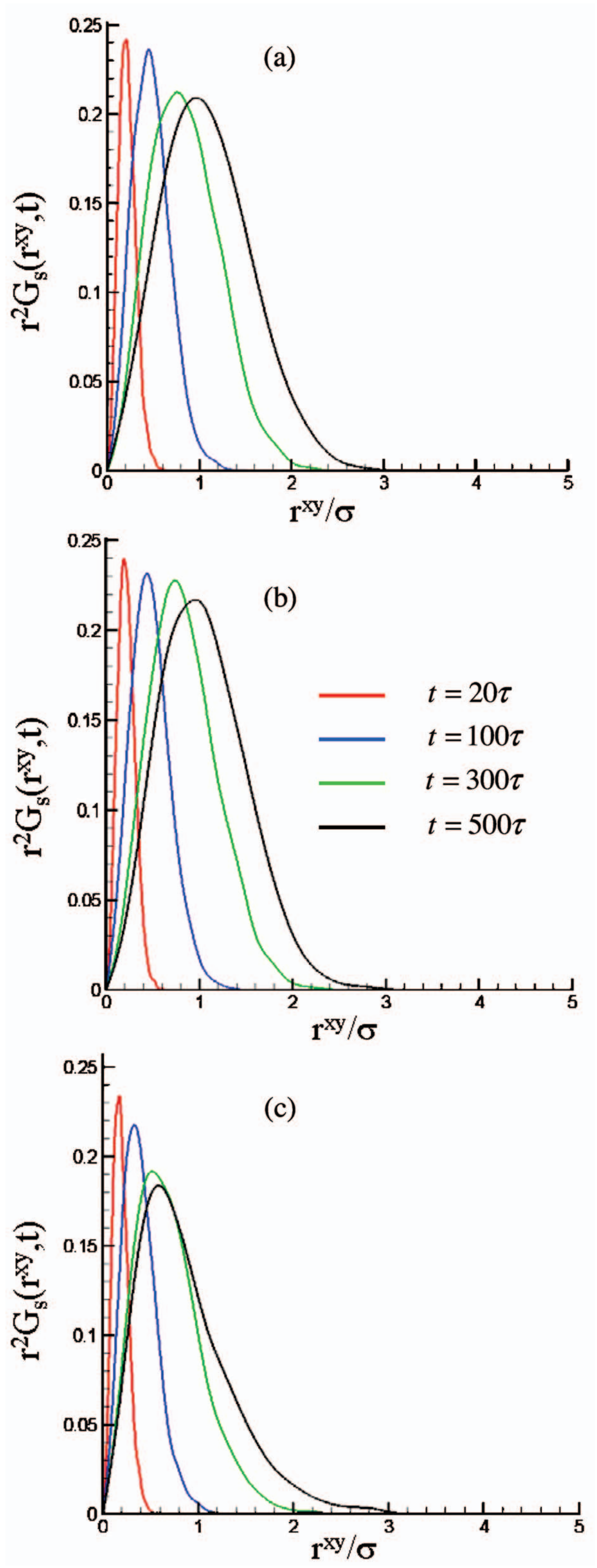

FIG. 1. (Color) Self space-time correlation function $G_s(r^{xy},t)$ multiplied by the displacement squared at four different times for the following nanofluid parameters: $\sigma=d=80$ nm, $h=7\sigma$, $\phi=1\%$, $r_c=1.5\sigma$, $T=300$ K, $\varepsilon=5\ k_BT$, $\tilde{\varepsilon}=0.01\ k_BT$, $\hat{\varepsilon}=\zeta k_BT$ with $\zeta=0.01$ (a), $\zeta=0.1$ (b), and $\zeta=1$ (c). Averages were computed over 900 time origins for five different initial distributions, each origin separated by 30 time steps. The delay time $\tau=8.88$ ns.

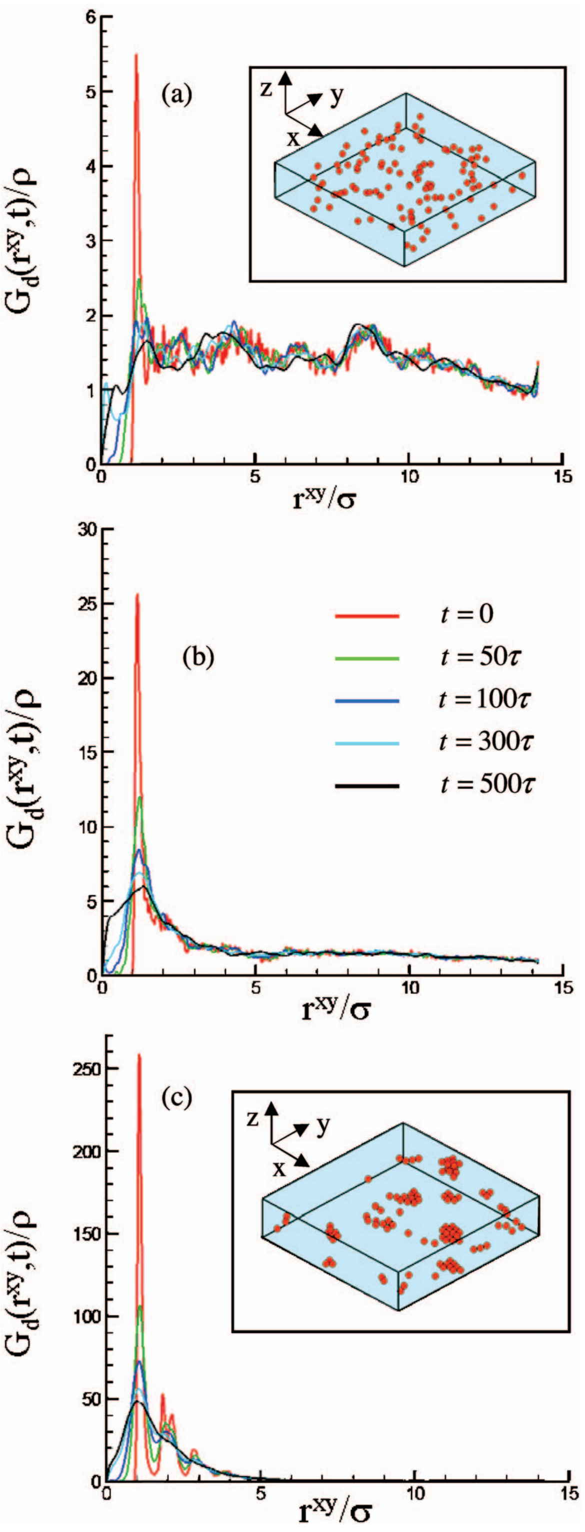

FIG. 2. (Color) Distinct space-time correlation function $G_d(r^{xy},t)$ divided by the ideal density $\rho=N/V$ at five different times for the following nanofluid parameters: $\sigma=d=80$ nm, $h=7\sigma$, $\phi=1\%$, $r_c=1.5\sigma$, $T=300$ K, $\varepsilon=5\ k_BT$, $\tilde{\varepsilon}=0.01\ k_BT$, $\hat{\varepsilon}=\zeta k_BT$ with $\zeta=0.01$ (a), $\zeta=0.1$ (b), and $\zeta=1$ (c). Averages were computed over 900 time origins for five different initial distributions, each origin separated by 30 time steps. The delay time $\tau=8.88$ ns. Insets: snapshot after equilibration (50 000 time steps more) of an instantaneous configuration. Lengths have been rescaled for readability reasons.

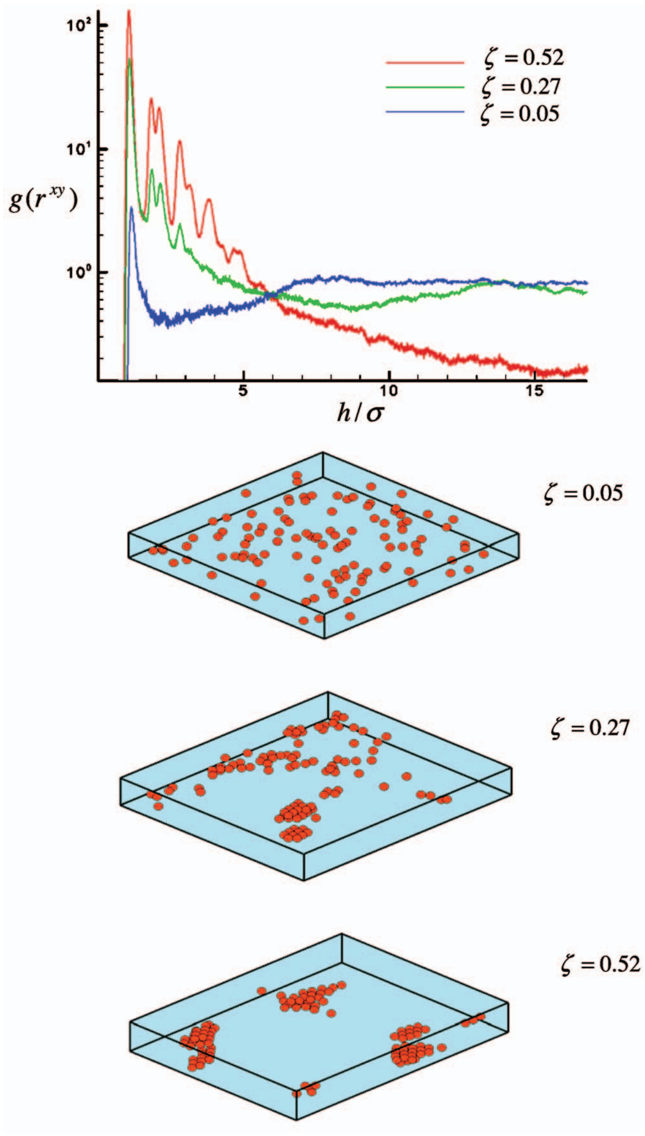

FIG. 3. (Color) Logarithmic plot of the longitudinal distribution function and the corresponding snapshots for nanoparticles confined between two parallel boundaries spaced by a distance $h=5\sigma$ and submitted to external perturbations several levels of magnitude [$\sigma=d=80$ nm, $\phi=1\%$, $T=300$ K, $\varepsilon=5\ k_BT$, $\tilde{\varepsilon}=0.01\ k_BT$, and $r_c=1.5\sigma$].

enough to avoid the finite-size effects we generally observe in bulk suspensions.

III. IN PLANE SELF-DIFFUSION

To study the correlation of a particle with itself during its motion in the x-y plane we calculate the correlation function which is formally defined as follows:

$$G_s(\mathbf{r}^{\mathbf{xy}},t) = \frac{1}{N}\left\langle \sum_i \delta(\mathbf{r}^{\mathbf{xy}} - \mathbf{r}_{\mathbf{i}}^{\mathbf{xy}}(0) - \mathbf{r}_{\mathbf{i}}^{\mathbf{xy}}(t)) \right\rangle. \tag{6}$$

At $t=0$ (this case is not plotted for readability reasons) each particle is δ correlated with itself so that $G_s(\mathbf{r}^{\mathbf{xy}},0)=\delta$. Then

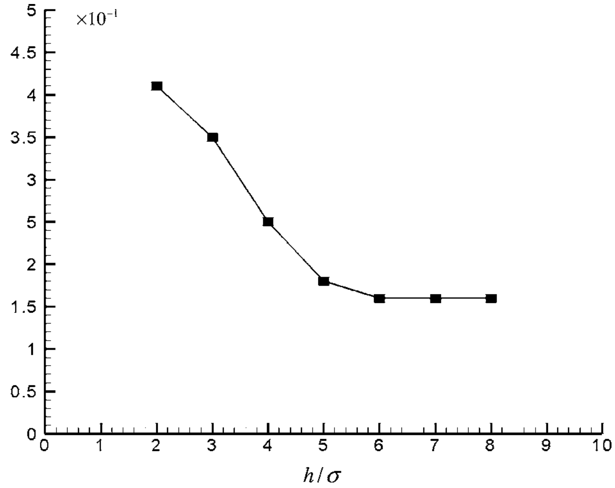

FIG. 4. Threshold strengths as function of the separation distance h [$\sigma=d=80$ nm, $\phi=1\%$, $T=300$ K, $\varepsilon=5\ k_BT$, $\tilde{\varepsilon}=0.01\ k_BT$, and $r_c=1.5\sigma$].

the self-component of the van Hove function spreads out with time as a result of particle self-diffusion. At long times and long distances the particles are uncorrelated so that we have $\lim_{r\to\infty} G_s(\mathbf{r}^{\mathbf{xy}},t)=\lim_{t\to\infty} G_s(\mathbf{r}^{\mathbf{xy}},t)=\frac{1}{V}\approx 0$, V being the volume of the simulation box. In Fig. 1 we see, for a given degree of confinement ($h=7\sigma$), that G_s spreads out more slowly as the magnitude of the external force field increases. This effect is more marked with more intense forces. Thus the external irradiation reduces the mobility of particles in the x-y plane as the confinement would do it. It restricts the number of freedom degrees for the particles and consequently lowers the probability of collisions which basically reduce the self-correlation of particles.

IV. DYNAMICS OF LONGITUDINAL COLLECTIVE MODES AND CLUSTERS FORMATION

To analyze in detail the behavior of collective modes in the x-y plane under the action of an external force field, let us now focus our attention on the distinct part of the van Hove function which is defined as follows: [15]

$$G_d(\mathbf{r}^{\mathbf{xy}},t) = \frac{1}{N}\left\langle \sum \sum_{i\neq j} \delta(\mathbf{r}^{\mathbf{xy}} - \mathbf{r}_{\mathbf{j}}^{\mathbf{xy}}(0) - \mathbf{r}_{\mathbf{i}}^{\mathbf{xy}}(t)) \right\rangle. \tag{9}$$

This function is simply the time correlation of distinct particles and hence informs us on the collective behavior of particles in the x-y plane. Figure 2 shows the evolution of $G_d(\mathbf{r}^{\mathbf{xy}},t)$ at successive time intervals for several particle sizes in a channel of width 7σ. At time $t=0$ the distinct part of the van Hove function is identical to the in plane pair distribution function modulo=the density of particles, i.e., $G_d(\mathbf{r}^{\mathbf{xy}},0)=\rho g(\mathbf{r}^{\mathbf{xy}})$. Close to contact, the height of the first peak of correlation increases considerably compared to that of the free system. This means that the external force field improves the structural order at short distance. Thus, this field makes the nanoparticles more attractive. One can also observe that the range of correlation increases with the magnitude of the field. The correlation length takes a value of about σ for $\zeta=0.01$ and it reaches approximately 5σ when $\zeta=1$. We see on the snapshot of nanoparticles (insets of Fig. 2), this result is closely related to the presence of strong heterogeneities and to the formation of nanoparticle clusters beyond many threshold strengths. A similar behavior has been observed in colloidal dispersions subject to high shear rates ("shear thickening" [16,17]). The presence of density inhomogeneities (a reminiscence of interparticle clusters) in unconfined binary mixtures in the presence of a strong external field also has been reported [18]. However, no analog result has been highlighted so far in strongly asymmetric mixtures (i.e., Brownian particles) under confinement. Here we observe different crystalline phases depending on the strength field. In Fig. 2 the evolution of the G_d curves is plotted from the time $t=0$ s to $t=500\ \tau$ for three different magnitudes of external strength. These curves give both qualitative and quantitative information about the lifetime of damped collective modes of particles (i.e., natural phonons) in the host fluid. At long time and large separation distances the correlation of distinct particles decreases so that $\lim_{r\to\infty}G_d(\mathbf{r}^{\mathrm{xy}},t)=\lim_{t\to\infty}G_d(\mathbf{r}^{\mathrm{xy}},t)=\rho$. In contrast at a short distance and a short time the G_d curves closely depend on the external perturbation. In Fig. 2 we see that the shell structure at short distance disappears more slowly with time as the magnitude of the external force field increases. Hence, we observe that two distinct particles of 80 nm become almost uncorrelated after a time interval of $300\ \tau$ when the magnitude of the field is equal to $\hat{\varepsilon}=0.1\ k_BT$. On the other hand, these particles remain correlated during a time interval greater than $500\ \tau$ when $\hat{\varepsilon}=k_BT$. This behavior essentially means that the external perturbation enhances the relaxation time of collectives modes which are less damped than without perturbation. This enhancement is related to significant changes in the spatial distribution of colloidal particles in the x-y plane. Indeed, in Fig. 3 we observe that the first peaks of the $g(r^{xy})$ curves become more pronounced as the magnitude of field increases. This is a clear indication of the shell structure formation in the x-y plane. Moreover, as the magnitude of the field increases, the particle distribution becomes more and more inhomogeneous and from a threshold strength ζ^* many nanoparticles clusters are formed in the host fluid. In Fig. 3. we see that these clusters growth monotonically with the magnitude of the field. The dependence of the threshold strength on the separation distance h between the walls also has been examined. Interestingly one remarks (Fig. 4) that this critical strength notably decreases with h showing that the interaction forces mediated by the walls act like repulsive interparticle forces. Therefore the confining walls limit the cluster formation and consequently lower the lifetime of collective modes which become less important than those observed in homogeneous three-dimensional colloidal systems. In Fig. 4 we see these effects are limited to strongly confined geometries. Beyond a critical separation distance, of the order of some particle diameters, the confining wall effects on the structural order become negligible. For instance, in a suspension of 80 nm particles dispersed at 1% vol. in a fluid with the same viscosity than ethylene glycol this critical distance is approximately equal to six diameters. Below this limit, the confining walls reduce the probability of cluster formation.

V. CONCLUSION

We have demonstrated that an external force field applied on confined nanofluids is able to reduce the nanoparticles' mobility and to significantly enhance the lifetime of natural phonons. This result is similar with that observed in colloidal suspensions under shear flow at high shear rates. It is related to disorder-order transitions in the nanoparticle distribution under perturbation. Interestingly, we have highlighted that the interaction forces mediated by the walls act like repulsive interparticle forces. They tend to increase the structural disorder and to lower the lifetime of collective modes. Our results suggest that the heat transport properties of nanofluids could be actively controlled in nanometer-size systems.

---

[1] J. A. Eastman, S. U. S. Choi, S. Li, W. Yu, and L. J. Thompson, Appl. Phys. Lett. **78**, 718 (2001).

[2] J. A. Eastman, S. R. Phillpot, S. U. S. Choi, and P. Keblinski, Annu. Rev. Mater. Res. **34**, 219 (2004).

[3] S. Lee, S. U. S. Choi, and J. A. Eastman, J. Heat Transfer **121**, 28 (1999).

[4] S. K. Das, N. Putra, P. Thiesen, and W. Roetzel, J. Heat Transfer **125**, 567 (2003).

[5] R. L. Hamilton and O. K. Crosser, Ind. Eng. Chem. Fundam. **1**, 187 (1962).

[6] P. Keblinski, J. A. Eastman, and D. G. Cahill, Mater. Today **8** 36 (2005).

[7] R. Prasher, P. Bhattacharya, and P. E. Phelan, Phys. Rev. Lett. **94**, 025901 (2005).

[8] M. Vladkov and J. L. Barrat, Nano Lett. **6**, 1224 (2006).

[9] P. Ben-Abdallah, Appl. Phys. Lett. **89**, 113117 (2006).

[10] A. Ashkin, J. M. Dziedzic, J. E. Bjorkholm, and S. Chu, Opt. Lett. **11**, 288 (1986).

[11] P. Ben-Abdallah, A. Ould El Moctar, B. Ni, N. Aubry, and P. Singh, J. Appl. Phys. **99**, 094303 (2006). See also N. Aubry and P. Singh, Europhys. Lett. **74**, 623 (2006).

[12] H. B. Callen and T. A. Welton, Phys. Rev. **83**, 1 (1951).

[13] D. L. Ermak and J. A. McCammon, J. Chem. Phys. **69**, 1352 (1978).

[14] J. Rotne and S. Prager, J. Chem. Phys. **50**, 4831 (1969).

[15] See, for instance, J. L. Barrat and J. P. Hansen, *Basic Concepts for Simple and Complex Liquids* (Cambridge University Press, London, 2001).

[16] M. C. Newstein, H. Wang, N. P. Balsara, A. A. Lefebvre, Y. Shnidman, H. Watanabe, K. Osaki, T. Shikata, H. Niwa, and Y. Morishima, J. Chem. Phys. **111**, 4827 (1999).

[17] B. Maranzano and N. J. Wagner, J. Chem. Phys. **117**, 10291 (2002).

[18] J. Delhommelle, Phys. Rev. E **71**, 016705 (2005). See also J. Delhommelle and J. Petravic, J. Chem. Phys. **123**, 074707 (2005).